Hindawi
Structural Control and Health Monitoring
Volume 2024, Article ID 3280697, 17 pages
https://doi.org/10.1155/2024/3280697

WILEY | Hindawi

Research Article

Identification Uncertainties of Bending Modes of an Onshore Wind Turbine for Vibration-Based Monitoring

Clemens Jonscher, Sören Möller, Leon Liesecke, Daniel Schuster, Benedikt Hofmeister, Tanja Grießmann, and Raimund Rolfes

Leibniz University Hannover, Institute of Structural Analysis, Appelstraße 9A, Hannover 30167, Germany

Correspondence should be addressed to Clemens Jonscher; c.jonscher@isd.uni-hannover.de

Received 7 December 2023; Revised 31 January 2024; Accepted 14 February 2024; Published 11 March 2024

Academic Editor: Łukasz Jankowski

This study considers the identification uncertainties of closely spaced bending modes of an operating onshore concrete-steel hybrid wind turbine tower. The knowledge gained contributes to making mode shapes applicable to wind turbine tower monitoring rather than just mode tracking. One reason is that closely spaced modes make it difficult to determine reliable mode shapes for them. For example, the well-known covariance-driven stochastic subspace identification (SSI-COV) yields complex mode shapes with multiple mean phases in the complex plane, which does not allow error-free transformation to the real space. In contrast, the Bayesian Operational Modal Analysis (BAYOMA) allows the determination of real mode shapes. The application of BAYOMA presents a further challenge when quantifying the associated uncertainties, as the typical assumption of a linear, time-invariant system is violated. Therefore, validity is not self-evident and a comprehensive investigation and comparison of results is required. It has already been shown in a previous study that the significant part of the uncertainty in the mode shapes corresponds to their orientation in the mode subspace (MSS). Despite all the challenges mentioned, there is still a great need to develop reliable monitoring parameters (MPs) for Structural Health Monitoring (SHM). This study contributes to this by analysing metrics for comparing mode shapes. In addition to the well-known Modal Assurance Criteria (MAC), the Second-Order MAC (S2MAC) is also used to eliminate the alignment uncertainty by comparing the mode shape with a MSS. In addition, the mode shape identification uncertainties of BAYOMA are also considered. Including uncertainties is also essential for the typically used natural frequencies and damping ratios, which can be more appropriately used if the identification uncertainty is known.

1. Introduction

Wind energy accounts for the largest share of renewable electricity generation in the European Union (EU). In 2018, wind energy accounted for 18.4% of the electricity generation capacity in the EU, with an installed capacity of 170 Gigawatt (GW) onshore and 19 GW offshore [1]. As in many engineering disciplines, efficient operation and maintenance also play a major role in the field of wind turbines. Therefore, there is a strong incentive to establish efficient monitoring strategies to minimise maintenance expenses whilst simultaneously enhancing safety [2]. In civil engineering, the associated monitoring concept is referred to as *Structural Health Monitoring* (SHM). A distinction between model- and data-based SHM in this context is generally made. In model-based SHM, a simulation model of a wind turbine is used, which can rely just on its structure model or can also consider the environment (like aerodynamics). Popko [3] presented an overview of commonly applied wind turbine simulation tools. For further SHM applications, the model must be accurate enough to reflect reality. On the one hand, this is achieved by calibrating the structural model. On the other hand, the model has to consider all relevant interactions accurately enough, such as soil-structure and fluid-structure interactions. Several studies investigate vibration and time simulations of onshore wind turbine simulations considering such interactions [4, 5]. Since this paper focuses on the identification of modal parameters

from measurement data considering the identification uncertainties, the model-based SHM is not in the scope of this work. However, we use a simulation model to generate data to preliminary investigate the identification of closely spaced modes of tower structures before using real measurement data.

For data-based methods, a suitable measurement concept is crucial. A global monitoring approach is often used due to a more economic measurement concept than local approaches. Here, a small number of sensors are used to determine information about the condition of the whole structure in terms of structural dynamics. Based on the measured system response data, monitoring parameters (MPs) are extracted using feature extraction techniques. From these parameters, a subset of parameters is determined which can distinguish between a damaged and an undamaged state of the structure [6]. Here, operational modal analysis (OMA) methods are often used to determine modal parameters such as natural frequencies, damping ratio, and mode shapes as MPs. This study aims to investigate the identification of modal parameters and their uncertainties as MPs for a hybrid concrete-steel tower in a 3.4 MW onshore wind turbine during operation. In the use case of wind turbine monitoring, the *Stochastic Subspace Identification* (SSI) [7–11], the *poly-reference Least Squares Complex Frequency* (pLSCF) [8, 9], and the *Frequency Domain Decomposition* (FDD) [12, 13] are to be mentioned here. In this application, a nonstationary, time-variant system is typically present, contradicting the assumption of a time-invariant system under white noise excitation of linear OMA methods.

In general, the difficulty in applying these methods lies in the complexity of a wind turbine. This complexity is manifested in identifying modal parameters in the presence of harmonic excitation, which can lead to distortion of the natural frequencies [7]. Possible approaches in the context of monitoring wind turbine towers, for example, do not consider the identified natural frequencies in the range of higher harmonics of the rotor [14], or use cluster analysis to separate natural frequencies from harmonics [15]. Another challenge arises from the short evaluation time compared to the oscillation period (typically 10 minutes). However, there arises also a problem if the evaluation time is extended beyond the commonly used 10 minutes to improve the identification accuracy because there is a risk that the identification will become less reliable due to instationarities caused by varying environmental and operating conditions (EOCs). Nevertheless, OMA methods are often successfully used to monitor and identify the dynamics of wind turbine support structures, as they are robust against violations of the assumptions [8, 16]. Identifying the dynamics of wind turbine towers is further complicated by the fact that the damping of the fore-aft mode (FA) at higher rotor speeds is greater than that of the side-to-side mode (SS) [12]. In addition, the damping of a hybrid tower is greater than that of a pure steel tower. The tower also has a greater mass, making the structure less susceptible to vibration than a typical steel tower. The low-frequency system dynamics are also challenging to capture. Therefore, the measurement chain must be designed and calibrated for the low-frequency range [17]. All these effects ultimately increase the identification uncertainty of the modal parameters [18].

In recent years, OMA methods, therefore, have focused on the consideration of uncertainties and methods such as Bayesian Operational Modal Analysis (BAYOMA) [19] or the uncertainty extension for the SSI [20] have been developed. Including those uncertainties is of great importance to monitor a wind turbine reliably. However, one of the main challenges with monitoring tower structures is still the identification of closely spaced modes, especially in terms of mode shapes. When applying the widely used SSI-COV to tower structures, the problem with closely spaced modes is that the identified complex mode shapes may have mean phases separated by spatial directions [21–23], making it difficult to compare the mode shapes. By contrast, BAYOMA can be used to identify real mode shapes and will, therefore, also be used in this study. Regarding uncertainty, Au et al. [18] showed that the largest uncertainty in the case of closely spaced modes occurs in the identified mode shapes. This uncertainty can be divided into two parts. The first part is the uncertainty of the mode subspace (MSS) spanned by the dominant vibration shapes. This uncertainty is similar to the uncertainty of mode shapes in the well-separated case, which depends mainly on the noise of the measurement chain. Hence, the MSS can be identified in the case of low-noise data very reliably. The second part of the uncertainty of the mode shape is the alignment of the mode in the MSS. This finding aligns with [21], which examines the mode shapes of a prestressed segmented concrete tower under laboratory conditions using BAYOMA and SSI-COV. It was found that the uncertainty of the alignment identification increases significantly with the increase in closeness of the frequencies. It has also been shown that an extension of the well-known modal assurance criterion (MAC) in the form of the subspace of order 2 MAC (S2MAC) [24] is advantageous in this case and enables the detection of system changes for symmetrical tower structures based on mode shapes [21, 25].

Therefore, this study aims to transfer the findings of the identification uncertainty of closely spaced modes [21] to monitor a hybrid tower of a 3.4 MW onshore wind turbine during operation. To achieve this, first, the SSI-COV and BAYOMA are compared using a simulation model of a tower. Subsequently, the suitability of BAYOMA to a wind turbine in operation is analysed, and the uncertainties associated with identifying the hybrid tower are investigated. Additionally, a new representation of the S2MAC is used to compare mode shapes of natural frequencies that are closely spaced. As a result, it can be demonstrated how to handle the mode shape uncertainty with meaningful metrics based on the MSS, particularly from closely spaced modes, to obtain a significant MP for the SHM of an onshore wind turbine. The work is structured as follows. Section 2 introduces the metrics considered in subsequent sections. Section 3 describes the investigated tower and the measurement setup. In Section 4, a comparison of the identification methods based on a simulation model of a tower is performed. Section 5 examines the wind turbine tower under investigation and analyses its dynamics in greater detail, accounting for

identification uncertainty. Lastly, Section 6 provides a summarised review of the study and offers an outlook.

2. Metrics for Mode Shapes

For almost rotationally symmetric tower structures, closely spaced modes occur for bending deformations since the natural frequencies of the two spatial bending directions are almost the same. In such cases, previous investigations have shown that the mode shapes have much higher associated identification uncertainty than in the case of well-separated modes [18, 25]. The widely used metric to compare to mode shapes $\boldsymbol{\varphi}_j$ and $\boldsymbol{\varphi}_k$ is the Modal Assurance Criterion (MAC), defined as

$$\mathrm{MAC}_{j,k} = \frac{\left|\boldsymbol{\varphi}_j^H \boldsymbol{\varphi}_k\right|^2}{\boldsymbol{\varphi}_j^H \boldsymbol{\varphi}_j \boldsymbol{\varphi}_k^H \boldsymbol{\varphi}_k}. \tag{1}$$

Most of the uncertainty is in the alignment of the mode shape in the MSS, so the MAC becomes very uncertain, as shown in [21, 25]. Figure 1 shows a MAC interpretation for the three-dimensional case.

The subspace of order 2 Modal Assurance Criterion (S2MAC) was developed [24] to eliminate the alignment uncertainty. The S2MAC calculates the best MAC between the mode shape $\boldsymbol{\varphi}_i$ and the MSS spanned by two vibration shapes vectors $\boldsymbol{\psi}_j$ and $\boldsymbol{\psi}_k$. In the case of normalised real mode shapes of length one, the S2MAC is defined as

$$S2\mathrm{MAC}_{i,jk} = \frac{\left(\boldsymbol{\varphi}_i^T \boldsymbol{\psi}_j\right)^2 - 2\left(\boldsymbol{\varphi}_i^T \boldsymbol{\psi}_j\right)\left(\boldsymbol{\psi}_j^T \boldsymbol{\psi}_k\right)\left(\boldsymbol{\varphi}_i^T \boldsymbol{\psi}_k\right) + \left(\boldsymbol{\varphi}_i^T \boldsymbol{\psi}_k\right)^2}{1 - \left(\boldsymbol{\psi}_j^T \boldsymbol{\psi}_k\right)^2}. \tag{2}$$

This metric determines the best possible MAC between the vector and a linear combination of two vectors, as visualised by a dashed red arrow in Figure 1. The MAC and S2MAC are relatively insensitive to small mode shape changes relative to the reference shape, respectively, MSS. Since both metrics represent a squared scalar product of vectors normalised to one, the corresponding angles α_{MAC} and $\alpha_{S2\mathrm{MAC}}$ can be derived [26].

$$\alpha_{\mathrm{MAC}} = \frac{180}{\pi} \arccos\left(\sqrt{\mathrm{MAC}}\right). \tag{3}$$

The angle of the MAC is simply the angle between the two mode shapes, and for the S2MAC, it is the smallest angle between the mode shape and the MSS, as shown in Figure 1. The representation using α_{MAC} and $\alpha_{S2\mathrm{MAC}}$ allows a more meaningful comparison of similar mode shapes. Moreover, a Gaussian distribution can better express the uncertainty distribution than without the angle transformation. Section 4 shows this fact in more detail.

The alignment in the MSS can be approximated by the directional angle γ in the case of a tower structure as visualised in Figure 1. If an orthogonal sensor setup at all measurement levels in both spatial directions exists, the directional angle is calculated analogous to the calculation of the mean phase [27], as shown in [21].

$$\gamma = \arctan\left(\frac{-V_{12}}{V_{22}}\right) \text{with } \mathbf{USV}^T = \left[\boldsymbol{\varphi}_x\ \boldsymbol{\varphi}_y\right], \tag{4}$$

where $\mathbf{USV}^T$ is the singular value decomposition, $\boldsymbol{\varphi}_x$ are the entries of the mode shape in x-direction, and $\boldsymbol{\varphi}_y$ are the entries of the mode shape in y-direction. V_{12} and V_{22} are the corresponding elements of the matrix $\mathbf{V}$. The alignment uncertainty in the MSS will be particularly noticeable in the directional angle for closely spaced modes. In the context of wind turbine towers, the directional angle depends on the nacelle position.

3. Case Study: 3.4 MW Onshore Wind Turbine Hybrid Concrete Steel Tower

This study investigates a hybrid concrete-steel tower of a 3.4 MW onshore wind turbine located close to Bremen, shown in Figure 2. The first 57 m of the 122 m high tower consists of prestressed segmented concrete rings. The upper part is composed of steel tubes.

The rated rotor speed of 14 rpm is reached at a wind speed of about 10 m/s. The main wind direction is west. Since the measurement system was installed on an existing wind turbine, the five measurement levels coincide with the tower platforms due to limited accessibility. Three *Integrated Electronics Piezo-Electric* (IEPE) accelerometers are installed on each level. Two sensors measure in the radial direction of the tower, with a 90° angle to each other (MP1r and MP2r). An additional sensor of tangential direction is attached to one measuring point (MP1t) per measuring level, as shown in Figure 2. The calibrated IEPE sensors are combined with an IEPE supply with a cutoff frequency of 0.0106 Hz, enabling the measurement of acceleration signals without distortion down to 0.05 Hz [17]. The measurement data of all sensors are digitised synchronously with a 24 bit analogue to digital converter on Level 1 positioned and stored on a computer with a sampling rate of 500 Hz. The signal is then digitally reduced to 10 Hz. This experimental setup aims to investigate the dynamics of the hybrid tower in operation to extract possible monitoring parameters and compare acceleration measurements with displacement measurements. In this work, the first is examined. For the evaluation, only the two accelerometers of MP1 from each measurement level are used.

4. Preinvestigations Using a Simulation Model

The findings of the investigations on the identification of closely spaced modes using BAYOMA and SSI-COV based on a laboratory structure [21] will first be verified in this section using a simulation model. This study does not describe the theory of the two identification methods. Interested readers are referred to the relevant literature for the SSI-COV [28, 29] and BAYOMA [30, 31].

The simulations are carried out in DeSiO, an in-house simulation tool for simulating slender structures prone to vortex-induced vibrations. It combines a structural model based on a multibody finite element system, possibly consisting of rigid bodies, geometrically exact beams and solid-

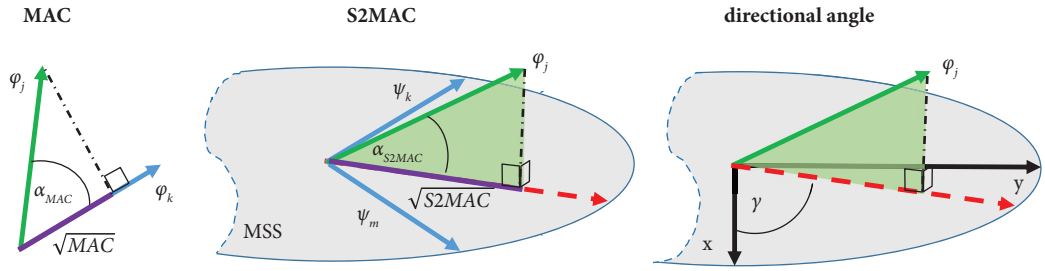

FIGURE 1: Visualisation of the metrics MAC, S2MAC, and directional angle for the three-dimensional case assuming that the alignment angle corresponds to the orientation of the mode in the MSS. Note the three-dimensional representation in the visualisation of the S2MAC and the directional angle.

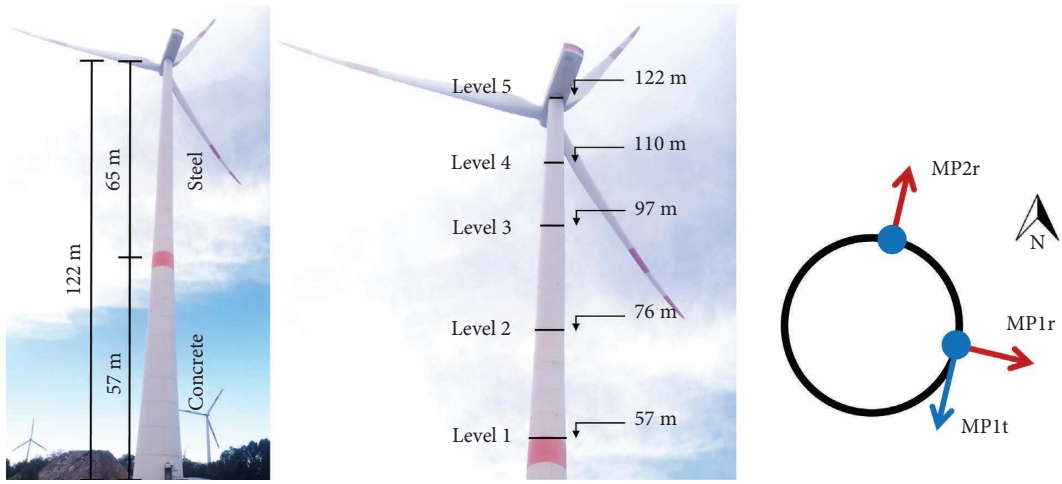

FIGURE 2: Sensor setup on the steel-concrete hybrid tower of a wind turbine. MP2 is aligned at 10° North and MP1 at 100° East.

degenerate shells, and the computation of aerodynamic loads by the unsteady vortex lattice method. The formulation allows using holonomic and nonholonomic constraint conditions [32]. In this work, only the structural solver is used. It combines a total Lagrangian formulation with a director-based description of the kinematics to ensure path independence and objectivity. Furthermore, the time integration methods allow for controlled energy dissipation but preserve total energy and linear and angular momentum [33]. Geometrically exact beam theory can be seen as an extension of the classical Timoshenko beam to geometric nonlinearity, allowing for the consideration of shear deformation as well as large rotations, large displacements, and coupled effects with regard to both stiffness and inertia.

The wind turbine tower described in Section 3 is modelled using one geometrically exact beam with a rigid body on top as a typical simplified model of the rotor nacelle assembly (RNA), i.e., nacelle, hub, and blades. The RNA is connected to the tower top knot by a set of constraints prohibiting any relative displacement and rotation. As no detailed information on the properties of these parts (especially of the blades) is available, the properties of this rigid body are chosen in a roughly realistic order of magnitude and in a manner that ensures that the slight asymmetry between the first FA and SS mode of the tower is captured. Since the focus of this work is not to simulate the wind turbine as realistically as possible but only for the validation of BAYOMA and SSI-COV, this is sufficient. The cross-sectional properties of the tower are modelled according to the provided documentation of its geometry and materials. The beam consists of 43 elements, with the bottom fixed rigidly on the ground. This simplification neglects the soil-structure interaction, as no foundation data and soil parameters were available. The top of the beam is rigidly connected to the rigid body, which represents RNA, as shown schematically in Figure 3. The different cross-sectional properties along the tower's height are considered by assigning different element mass and stiffness properties. More detailed information about the geometry and material parameters is subject to confidentiality.

Two types of simulations are carried out to compare the two OMA methods using the first pair of bending modes: firstly, a linear modal analysis, i.e. the classical eigenvalue problem neglecting all damping effects, is conducted to obtain the natural frequencies (details on the modal solver used in DeSiO can be found in [34]). As the deformation of the tower observed here is relatively small, this linear analysis is sufficiently accurate. The results are listed in Table 1 as "DeSiO." Figure 3 shows the corresponding first bending mode shape. Secondly, a transient simulation with

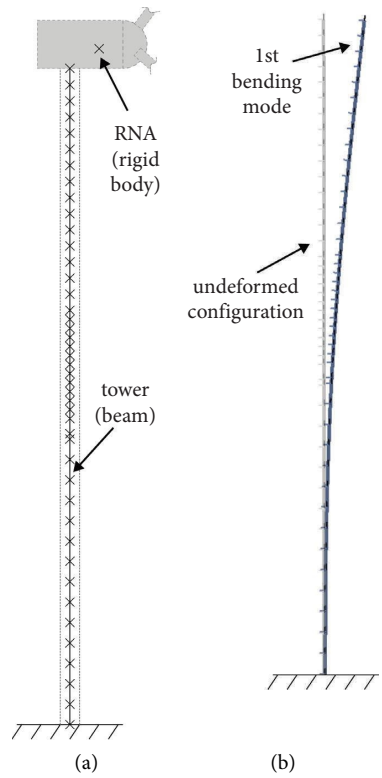

Figure 3: (a) A sketch of the FEM model of the wind turbine used in DeSiO (crosses correspond to the boundary of the elements). (b) Undeformed configuration and first bending mode of the tower (deformation scaled by factor 10 for better visibility).

Table 1: Natural frequencies f_0, the damping ratio ζ of the simulation model, and the identification results of BAYOMA or the SSI-COV.

Method	f_0 in Hz		ζ in %	
	$B1_y$ (CoV)	$B1_x$ (CoV)	$B1_y$ (CoV)	$B1_x$ (CoV)
DeSiO	0.2973	0.3021	*	*
BAYOMA	0.2975 (0.10%)	0.3021 (0.20%)	0.13 (139.3%)	0.35 (61.8%)
SSI-COV	0.2974	0.3017	0.20	0.11

The CoV in % is shown in brackets for the BAYOMA identification results (*since DeSiO includes only velocity damping but not modal damping, no equivalent damping ratio can be determined, for details, see [34]).

a duration of 10 minutes and a random excitation in the range of zero to two MN at the rigid body representing the RNA in all three spatial directions (i.e., vertical and in two perpendicular horizontal directions) is run to create the database for the analysis using BAYOMA and SSI-COV. This random excitation is used instead of computing aerodynamic forces. As we do not have detailed information on either the blade geometry or the wind loads acting on the turbine, simulating the aerodynamic loads in a meaningful way was not possible. However, only its structural response is required to identify the modal parameters of the tower. Therefore, we are able to use this random excitation instead. The resulting displacements are the same magnitude as those measured with terrestrial laser scanning at this wind turbine [35]. The corresponding identified natural frequencies f_0 and damping ratios ζ are also presented in Table 1. The same measurement levels are used for the identification procedure as for the real measurement.

As observed in previous studies [21, 36], the identified natural frequencies of both methods are almost identical under ideal conditions. The damping ratios are lower than those of a real wind turbine, which are around 1% [37] to allow using the linear modal solver to compare the identification results of BAYOMA and the SSI-COV with DeSiO. The reason for this underestimation is the neglect of the exact material damping and damping from the soil-structure interaction and aerodynamics. These topics will be addressed in future studies. For the investigations of the identified mode shapes, the mode shapes of the FE model are used as reference MSS and compared using the metrics presented in Section 2. The identification with BAYOMA provides the most probable values of the mode shape and the covariance matrix of the mode shape. The uncertainty of the metrics can be calculated using a Monte Carlo simulation with 3000 samples. The SSI-COV implementation that is used provides the most probable values so that one value can be calculated

for each metric, which is called deterministic. Real mode shapes are required to determine the S2MAC and the direction angle. Therefore, for the metrics, the mode shapes identified with SSI-COV are rotated by the mean phase in the complex plane, and then the real part is used. This procedure is equivalent to the complex normalisation used in [11]. For comparison, the metrics are also calculated deterministic using the most probable mode shape identified using BAYOMA. The results are shown in Figure 4.

The scatter of the MAC is shown in Figure 4(a). The result confirms previous studies [21, 25] that for tower structures the MAC becomes very uncertain for closely spaced modes. Moreover, no Gaussian distribution can be assumed when the MAC approaches one. The assumption of a beta distribution is better suited to modelling the MAC distribution [21]. Using a MSS as a reference and the S2MAC as metric, the scatter is significantly reduced compared to the regular MAC and the distribution is closer to a Gaussian distribution, as shown in Figure 4(c). However, a slight skewness of the distribution is still present. By the angular transformation S2MAC, α_{S2MAC} becomes Gaussian distributed, which is shown in Figure 4(d). In Figure 4(b), α_{MAC} illustrates that the angle representation can contain a deviation from the Gaussian distribution close to zero because the angles are constrained to be larger than 0. This error occurs in the case of large uncertainty and mean values close to 0, especially with the significantly less reliable α_{MAC}. The distribution of the direction angle in Figure 4(e) demonstrates clearly that it can be assumed as Gaussian. The comparison of the deterministic results of SSI-COV and BAYOMA does not show a clear result for the MAC and direction angle, as depending on the mode, a different identification method fits the simulation results better. Considering the S2MAC, the modes identified with BAYOMA are more suitable to the simulation model than those of SSI-COV. One reason for the differences in the identification of the mode shapes is the complex mode shapes of the SSI-COV with several mean phases according to spatial directions, as shown in Figure 5. This phenomenon in connection with closely spaced modes has already been observed in previous studies [21, 23].

The following section examines whether the findings from the simulation can be transferred to a real monitored wind turbine tower.

5. Structural Dynamics of the Tower

In this section, we first briefly examine the dynamics of the tower using a dataset as an example. Subsequently, the long-term behaviour of the dynamics of the tower is investigated. The dynamics of the tower are examined in more detail using the example of the 10-minute measurement dataset from 10/22/2021 at 3 p.m. with a wind speed of 11.23 m/s, a rotor speed of 13.7 rpm, and a nacelle position of 291°, which was the first one at rated speed. The singular value curve of the spectral matrix for this dataset is shown in Figure 6.

For using BAYOMA, the identification ranges must be defined in advance. Four bending mode pairs occur in the frequency range of up to 5 Hz. The identification ranges for these mode pairs are shown in Figure 6. In addition, the identification is also carried out for the dataset using the SSI-COV. The stabilisation diagram of the dataset is shown in Figure 6. A multistage clustering algorithm makes the mode selection [27]. The identified natural frequencies of the bending mode pairs for both identification methods are listed in Table 2. Both methods deliver similar results, as already shown in the previous section.

In addition to the modes described, the SSI identified further modes that are not considered in this study.

The mode shapes of BAYOMA-identified modes are shown in Figure 7.

The bending modes are similar in the FA and SS directions, respectively. The slight deviations may result from an asymmetric stiffness distribution around the circumference of the tower or the unevenly distributed head mass through the rotor and nacelle. The MSSs identified by the four bending mode pairs are used in the following as reference MSSs for the mode tracking and for the calculation of MAC and S2MAC.

To further examine the metrics introduced in Section 2 to compare the identified mode shapes with the reference ones in the context of the tower under investigation, the identified first FA bending mode of the following ten-minute dataset with similar operating conditions is used. This bending mode is closely spaced with the SS mode. The metrics results are shown the same way as for the simulation in Figure 8.

The distributions are similar to the simulation. However, in this case, α_{MAC} is significantly more Gaussian distributed, as the error close to zero is significantly lower. In addition, it is remarkable that the standard deviation of α_{MAC} and the direction angle are quite similar. This similarity indicates that the alignment uncertainty of the mode in the MSS is well described by the directional angle γ in the case of bending modes of the tower structures. The comparison of the mode shapes between the identification methods clearly shows that the mode shape identified using the SSI-COV fits better with the previously identified modes with the MAC. In contrast, the similarity with the BAYOMA-identified mode shapes is greater when using the S2MAC. This difference could be due to errors in transforming the complex modes of the SSI-COV into real space. A more detailed comparison of the two methods is not the scope of this work but will be pursued in the future.

The following investigation uses the BAYOMA identification method to study the long-term behaviours. The uncertainties of the mode shape metrics are determined with a 3000-sample Monte Carlo simulation, which considers the covariance matrix of the mode shape identification. The distribution of the mode shape metrics α_{MAC}, α_{S2MAC}, and γ is assumed to be Gaussian despite the possible small error. A mode tracking algorithm is required to determine the long-term dynamics, which is described in the following section.

5.1. Mode Tracking of Closely Spaced Modes. In the case of changing modal parameters caused by varying EOCs or mechanical changes, mode tracking becomes a challenge.

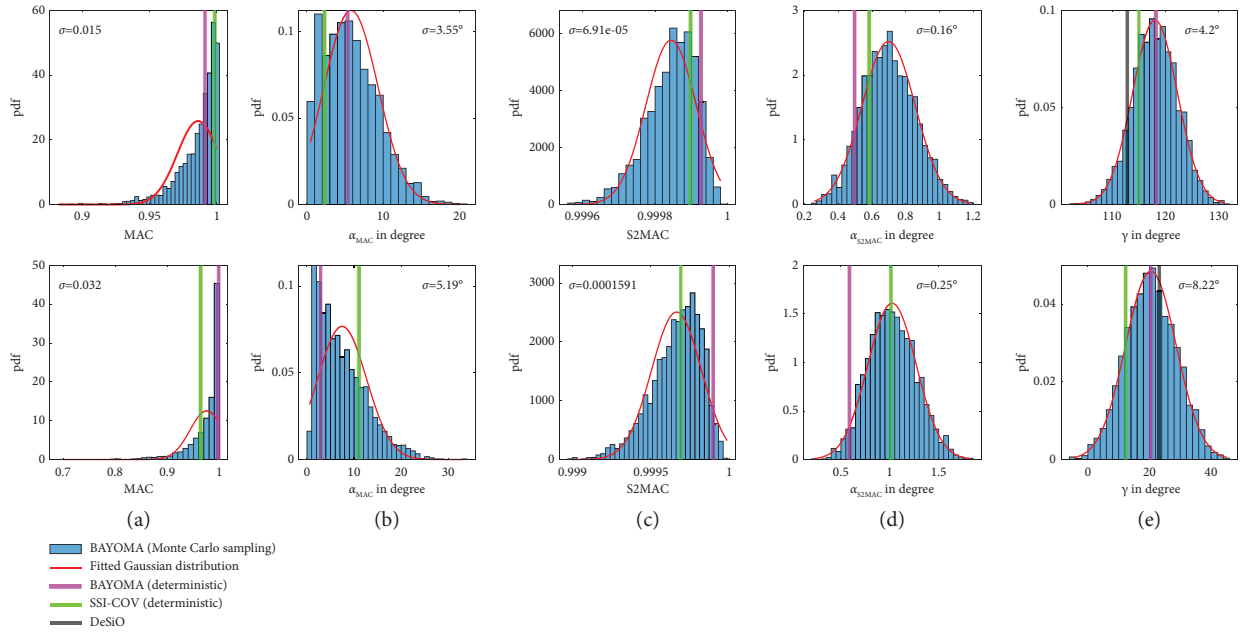

FIGURE 4: Histograms with normal distribution fits and the standard deviation σ of the MAC, α_{MAC}, S2MAC, α_{S2MAC}, and the directional angle γ of $B1_y$ (top line) and $B1_y$ (bottom line) identified mode shapes using SSI-COV and BAYOMA compared with the mode shapes of the DeSiO model, normalised according to the probability density functions (pdf). The determination of the uncertainty quantification of BAYOMA is performed using the covariance matrix of the mode shape and the Monte Carlo method with 3000 samples.

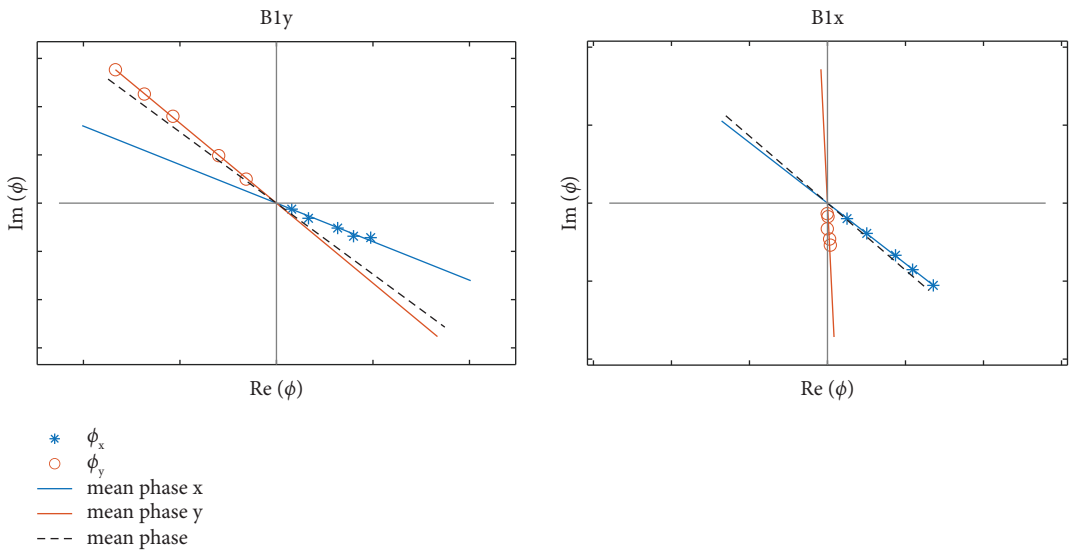

FIGURE 5: Visualisation of the mode shapes identified using the SSI-COV in the complex plane with coloured spatial directions. In addition, the mean phases of all sensors and the spatial directions are shown.

Here, the identified natural frequencies and mode shapes are compared with reference frequencies and reference shapes. An assignment of mode shapes in the presence of closely spaced modes is associated with significant uncertainties. In the case of support structures of wind turbines, this is further complicated because the mode alignment changes along with changing nacelle positions. A typical approach for this application is to rotate the reference mode shape depending on the nacelle position [15]. Subsequently, the rotated reference mode shape can be compared to the identified mode with the MAC, such that it becomes insensitive to the nacelle angle. A similar procedure is used for this study, shown in Figure 9.

First, the modal parameters and the associated uncertainties are identified from the acceleration measurement data using BAYOMA. Since BAYOMA is a nonparametric identification method, the identification ranges and the number of modes within a frequency range are required as prerequisite information. According to Brincker et al. [38], this information can be provided automatically or manually.

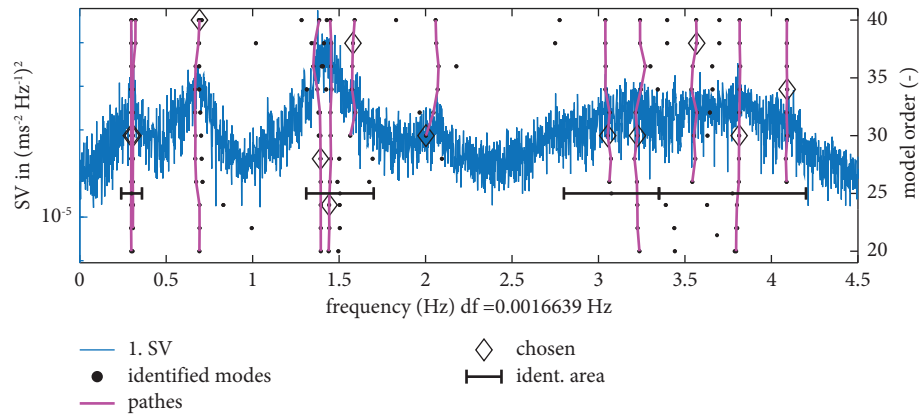

Figure 6: Stabilisation diagram with the first singular value (SV) of the spectrum of the identification with SSI-COV and the identification areas (ident. area) for the identification using BAYOMA of the dataset from 10/22/2021 at 3 p.m.

Table 2: Identification results of the natural frequencies f_0 of the four lowest bending mode pairs identified with BAYOMA and SSI-COV.

Mode pair	BAYOMA		SSI-COV	
	f_0 FA (CoV)	f_0 SS (CoV)	f_0 FA	f_0 SS
1	0.30 Hz (9.36%)	0.297 Hz (0.27%)	0.308 Hz	0.298 Hz
2	1.431 Hz (0.34%)	1.418 Hz (0.22%)	1.442 Hz	1.393 Hz
3	3.187 Hz (0.83%)	3.027 Hz (0.2%)	3.225 Hz	3.053 Hz
4	3.55 Hz (0.34%)	3.796 Hz (0.26%)	3.568 Hz	3.813 Hz

The coefficient of variation (CoV) is listed in brackets in BAYOMA in addition to the identifications.

In this work, the identification ranges are set manually. This manual setting has the advantage that only the modes of interest are identified. However, care must be taken to ensure that these ranges are sufficiently large to include the full range of variability and that the identification results are verified. For verification that two different modes have been identified, it is required that the maximum MAC of the two closely spaced mode shapes does not exceed 0.5 to obtain two different modes and that the identified natural frequencies are within the identification range.

In a further part of the verification, the S2MAC is used to check whether the identified mode matches the previously determined reference MSS. Assuming that the MSS of each bending mode pair identified with BAYOMA does not change significantly due to different EOCs, the identified MSS from the first dataset investigated in the previous section is used as the reference mode. The use of the S2MAC has the advantage that the alignment of the mode shape in the MSS, which is the main uncertainty of the mode shape for closely spaced modes, does not influence the mode tracking process. In addition, the influence of the nacelle position on the bending mode pair tracking can be eliminated, which is advantageous in the case of nonsynchronous aggregated *Supervisory Control and Data Acquisition* (SCADA). An identified mode is assigned to a bending mode pair when the S2MAC is higher than 0.8. Lower values of S2MAC are considered to be misidentifications.

However, the nacelle position is required to distinguish the modes according to FA and SS within a bending mode pair. This distinction is achieved by classifying the mode whose directional angle γ is closest to the nacelle position as the FA mode. The other mode is correspondingly assigned as the SS mode.

5.2. Long-Term Behaviour of the Tower Dynamics. For a detailed study of the long-term behaviour of the dynamics of the tower, measurement datasets from the middle of October 2021 to the end of September 2022 are used, assuming enough EOC variation during this period. Figure 10 shows the trend of the natural frequencies over time.

As generally known, the natural frequencies of wind turbine tower structures change over time due to EOCs. In addition, there appear to be assignment issues, especially with the second and fourth mode pair. A better insight is provided by the Campbell diagram in Figure 11, which shows the natural frequencies as a function of rotor speed.

The harmonic excitation has no relevant influence on identifying the modal parameters, as the dashed lines of the higher harmonics of the rotor speed do not correlate with the identified natural frequencies. In addition, the assignment problem of the fourth bending mode pair mainly occurs in standstill and start-up conditions. However, the second bending mode pair around 1.5 Hz scatters clearly and appears to have different states, as depicted in the Campbell diagram. Hence, the assignment of the second bending mode pair does not work reliably. A cause for this behaviour could not be found. However, interactions with the rotor may be an explanation. This theory is also supported by the fact that the SSI in Figure 6 identified another mode in this frequency range. However, this phenomenon deserves further investigation in future studies.

In the following, this study focuses on the dynamics of the plant in operation. To exclude uncertainties due to transient time signals caused by the start-up and shutdown of the wind turbine as far as possible, only datasets where the aggregated 10-minute SCADA data indicate constant

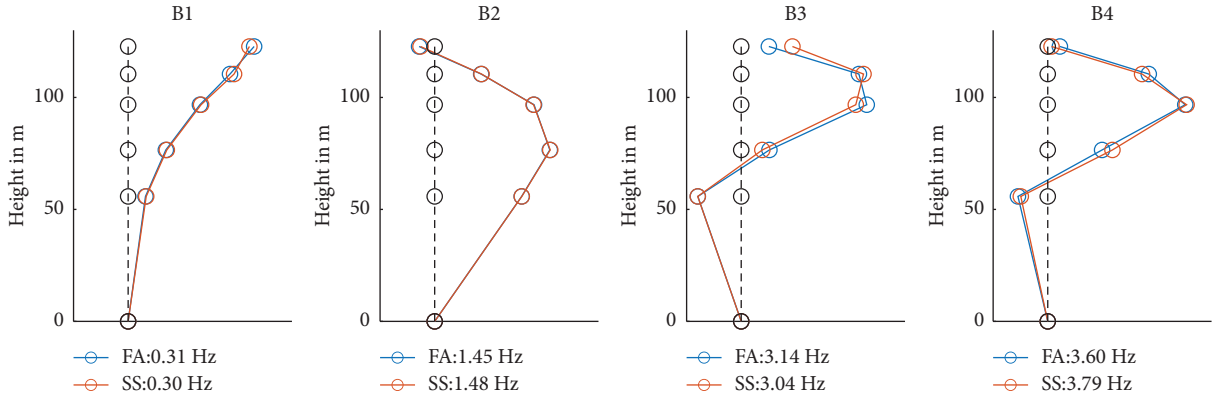

FIGURE 7: Mode shapes of the four bending mode pairs, identified under operation at a nacelle position of 270°, and rotated in the dominant direction for comparability.

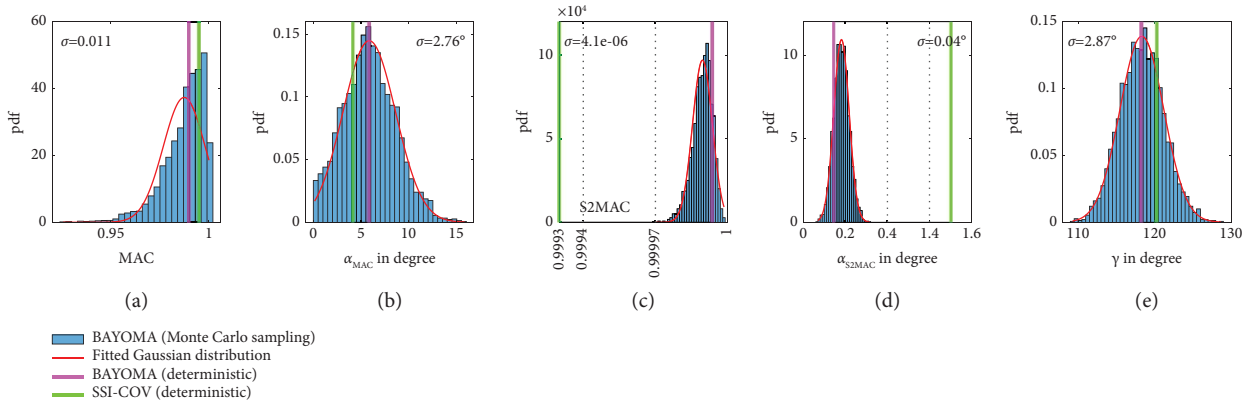

FIGURE 8: Histograms with normal distribution fits and the standard deviation σ of the MAC, α_{MAC}, S2MAC, α_{S2MAC}, and the directional angle γ of $B1_{\mathrm{FA}}$ mode shape of the dataset 10/22/2021 at 3.10 p.m., normalised according to the probability density function (pdf). The determination is performed using the covariance matrix of the mode shape and the Monte Carlo method with 3000 samples. Note the x-axis of the S2MAC and α_{S2MAC}.

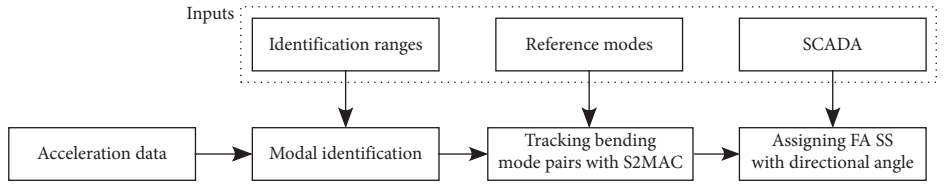

FIGURE 9: Sequence of identification and mode tracking used to monitor the support structure of a wind turbine.

operation are considered. Table 3 lists the selection criteria ensuring this. The medians of the identified natural frequencies and the identification rate for the selected data are listed in Table 4.

The reason for the relatively low identification rates is that only completely identified bending mode pairs are used. In the case of strongly unequal excitation of the pair, only one mode may be identified, and the identification of the pair is thus incomplete. In addition, harmonic excitation and other transient effects can disturb the identification, as in the case of the second bending mode. In general, some modes are often more difficult to identify when monitoring wind turbine towers [15], leading to lower identification rates. Figure 12 shows the power curve, the distribution of the wind speed and the wind direction of all data, and the selected data during the almost 12-month period considered in this study.

As stated before, only datasets belonging to operation conditions are used, and data points outside the expected power curve are not considered. Regarding the wind speeds, datasets below 2.7 m/s are consistently omitted. Otherwise, the distributions of wind speeds and wind direction remain qualitatively the same. For excluding inconclusive identification results, identifications are not considered if the

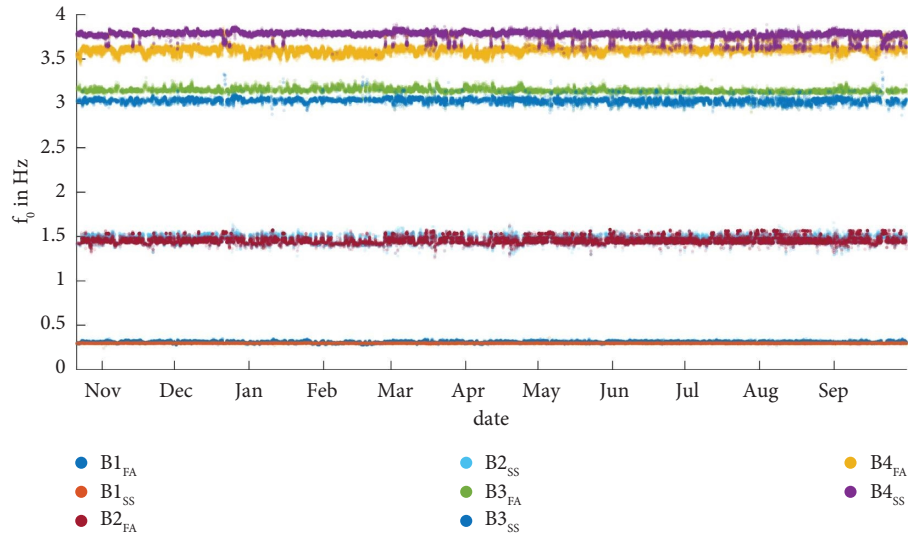

Figure 10: The natural frequencies of the four identified mode pairs plotted over time.

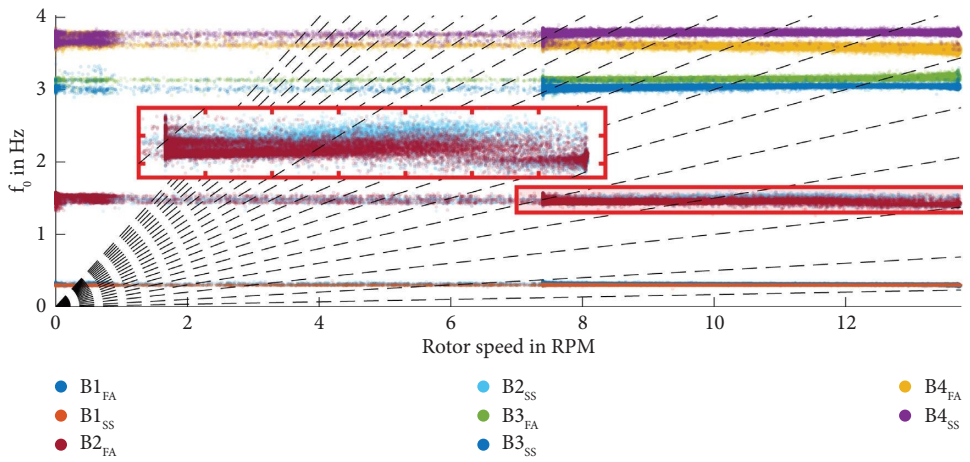

Figure 11: Campbell diagram with the natural frequencies of the four lowest bending mode pairs.

Table 3: Data selection criteria based on 10 minutes aggregated SCADA data.

Criterion	Minimum	Maximum	Max standard deviation
Power in kW	0	—	—
Pitch angle in degree	−2	25	2.5
Nacelle angle in degree	—	—	0.3

Table 4: Median of the natural frequencies f_0, identification range, and identification rate of the studied bending mode pairs for the selected EOCs from the middle of October 2021 to the end of September 2022.

Mode pair	f_0 FA (Hz)	f_0 SS (Hz)	Identification range (Hz)	Identification rate (%)
1	0.309	0.297	0.24 Hz–0.36	61.9
2	1.445	1.475	1.25 Hz–1.7	40.9
3	3.144	3.036	2.8 Hz–3.35	54.5
4	3.602	3.788	3.35 Hz–4.2	78.5

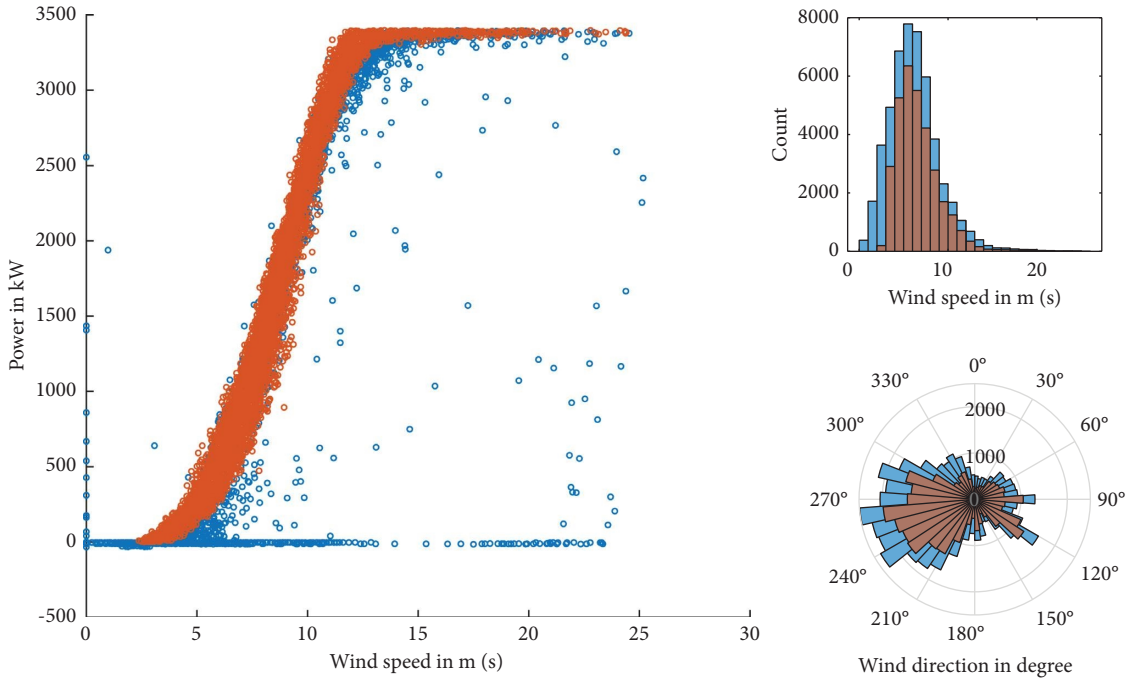

FIGURE 12: Power curve, wind speed, and wind direction distribution of the investigated wind turbine; blue: all data; red: selected data (October 2021–September 2022).

determined identification uncertainty of the natural frequency and damping ratio is detected as an outlier using a Hampel filter [39] with a window length of 144, which corresponds to one measurement day.

For further investigations, the first and fourth bending mode pairs are selected, as the first is the closest and the fourth is the best-separated mode pair. Figure 13(a) shows the natural frequencies depending on the wind speed. The first bending mode in the FA direction has a much stronger dependence on wind speed than the mode in the SS direction. In addition, the observed scattering of the FA direction is significantly higher. Similar observations are made for the fourth bending mode pair, although the scattering is lower than that for the first bending mode pair. The identification uncertainty of the natural frequencies in Figure 13(b) shows that the FA direction is identified with a higher uncertainty than the SS direction. The main reason for this difference is the aerodynamic damping [15], which leads to a significantly higher damping ratio in the FA direction, as shown in Figure 14.

A higher damping ratio leads to higher identification uncertainties of the frequency. Since the damping ratio of the first FA bending mode increases with the wind speed, the identification uncertainty of the natural frequency also increases. For the fourth bending mode pair, the highest damping ratio is determined between wind speeds of 4 and 12 m/s, so the corresponding natural frequencies are identified with the highest uncertainty in this range. In general, the identification of the damping is associated with significantly higher uncertainties than the identification of natural frequencies [40], and this can also be confirmed for the datasets used in this study. Regarding the uncertainties of the damping ratio identification, as shown in Figure 14(b), it is noticeable that the damping ratio identification of the SS modes is relatively more uncertain than the damping ratio identification of the FA modes. However, the absolute uncertainty of the damping ratio of the SS modes is still significantly lower than that of the FA modes. In addition, the damping ratio of the fourth bending mode pair can be identified more reliably than the damping ratio of the first mode pair. This effect is due to the length of the 10-minute datasets used. With increasing vibration periods in the 10-minute interval, the damping ratio identification becomes less uncertain. The uncertainty of the first bending modes in the SS direction is remarkable, as the identification uncertainties of the damping ratio are more scattering at wind speeds below 10 m/s, as opposed to the trends observed for the other modes.

In identifying closely spaced modes, the mode shapes are of particular interest. The main uncertainty concerns the alignment of the mode shape in the MSS. In the case of wind turbine towers, the mode shape also changes due to the nacelle position. Therefore, in Figure 15(a), α_{MAC} for both pairs of modes is shown as a function of the nacelle position. The reference modes have been identified in the main wind direction at a nacelle position of 270°, so at that nacelle position, the α_{MAC} value is close to 0. Due to the wind direction distribution, there are few measurement datasets at nacelle positions below 100° and above 320°. The deviation between the mode pairs depending on the nacelle position that can be observed in Figure 15 is due to the asymmetric stiffness distribution around the circumference, which may result from imperfections in the dry joints between the concrete segments or attachments.

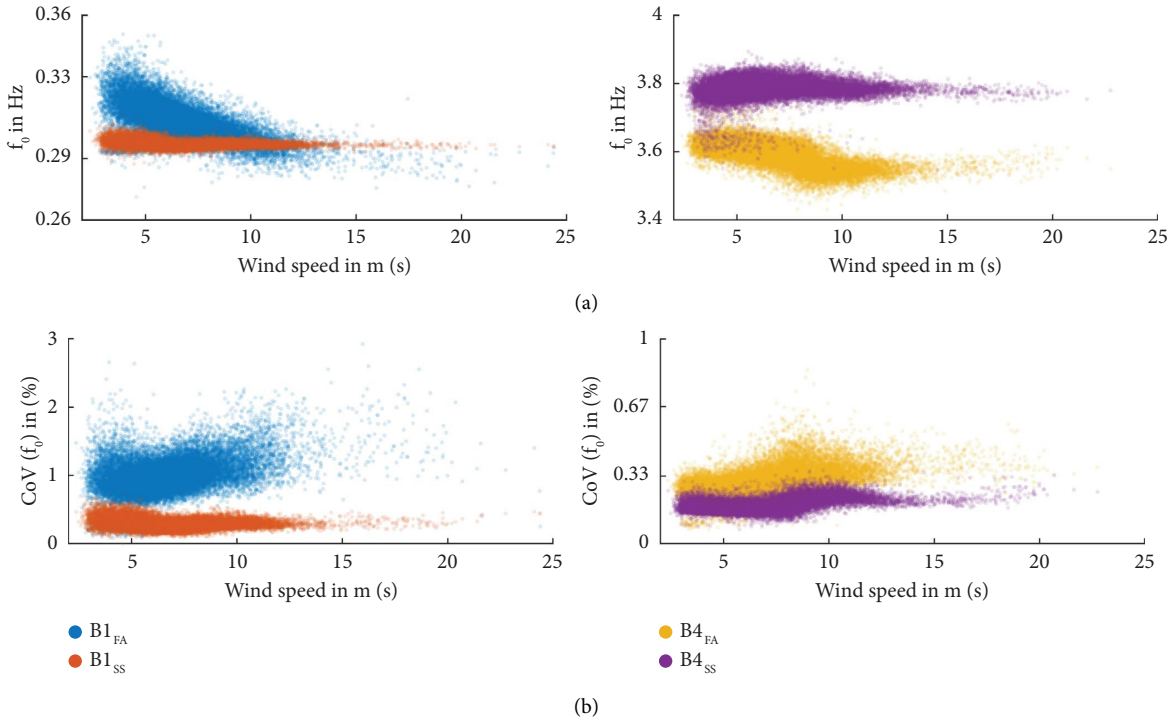

FIGURE 13: (a) Natural frequencies of the first and fourth bending mode pairs as a function of wind speed. (b) Coefficient of variation (CoV) of the natural frequencies as a function of wind speed.

The uncertainty of α_{MAC} is shown as a function of the wind speed. The fourth pair of bending modes is already well separated, so the uncertainty of α_{MAC} is relatively small, which leads to a standard deviation of the direction angle of less than 5° for both bending modes. In the case of the first bending mode pair, the standard deviation of the α_{MAC} is very high at low wind speeds, especially for the SS mode.

In contrast, α_{S2MAC} depicted in Figure 16 changes less depending on the nacelle position. In particular, the first bending mode pair appears to have a relatively constant α_{S2MAC} regardless of the nacelle position. The fourth bending mode pair has a clear dependence of α_{S2MAC} on the nacelle position. This dependency indicates that the MSS changes slightly as a function of the nacelle position, presumably due to an asymmetric stiffness distribution over the circumference. The uncertainties of α_{S2MAC} in Figure 16 are much lower than those of α_{MAC} in Figure 15 for both bending mode pairs. This observation indicates that α_{S2MAC} eliminates the alignment uncertainty. Furthermore, the uncertainty of α_{S2MAC} of the first bending mode pair is significantly lower than that of the fourth one. One reason could be a better signal-to-noise ratio, as has already been shown in [25]. In addition, the mode shape of the first bending mode pair has no nodal points at the sensor points considered, in contrast to the fourth bending mode pair, so the measurement noise has a minor influence.

The direction angle γ expresses the alignment of the mode shape in the MSS for symmetrical tower structure [21] and is shown in Figure 17. The closer the modes are to each other, the greater the uncertainty of the directional angle γ.

As expected, the direction angle γ in Figure 17(a) depends linearly on the nacelle position. However, a larger scatter can be observed over the whole trend. This scatter is due to the nonsynchronous SCADA and the uncertainty of the direction angle shown in Figure 17(b). The uncertainty is presented as a function of the wind speed. Considering this result, it is noticeable that the uncertainty of the direction angle is similar to the uncertainty of α_{MAC} in Figure 15. This fact demonstrates that the main uncertainty of the mode shapes of bending modes of wind turbine support structures originates from the alignment uncertainty within the MSS.

Throughout this investigation, it must be considered that the assumptions of BAYOMA, such as white noise as an excitation source and a linear time-invariant system, are violated. Therefore, the calculated uncertainties are indicative but do not precisely correspond to the actual uncertainties. However, for practical application, it can be stated that BAYOMA can be used to obtain consistent dynamical identifications of an onshore wind turbine tower.

Based on this investigation, it can be concluded that α_{MAC} of the tower bending mode shapes with their high identification uncertainties independent of the nacelle position cannot serve as a reliable monitoring parameter. Instead, the identified mode shapes should be compared with a MSS using α_{S2MAC}. This metric eliminates the high alignment uncertainty. As known from other studies [15], the more weakly damped SS natural frequencies can be identified more reliably than the FA natural frequencies. Nevertheless, it is recommendable to also consider the natural frequencies as monitoring parameters, like [9, 15, 41].

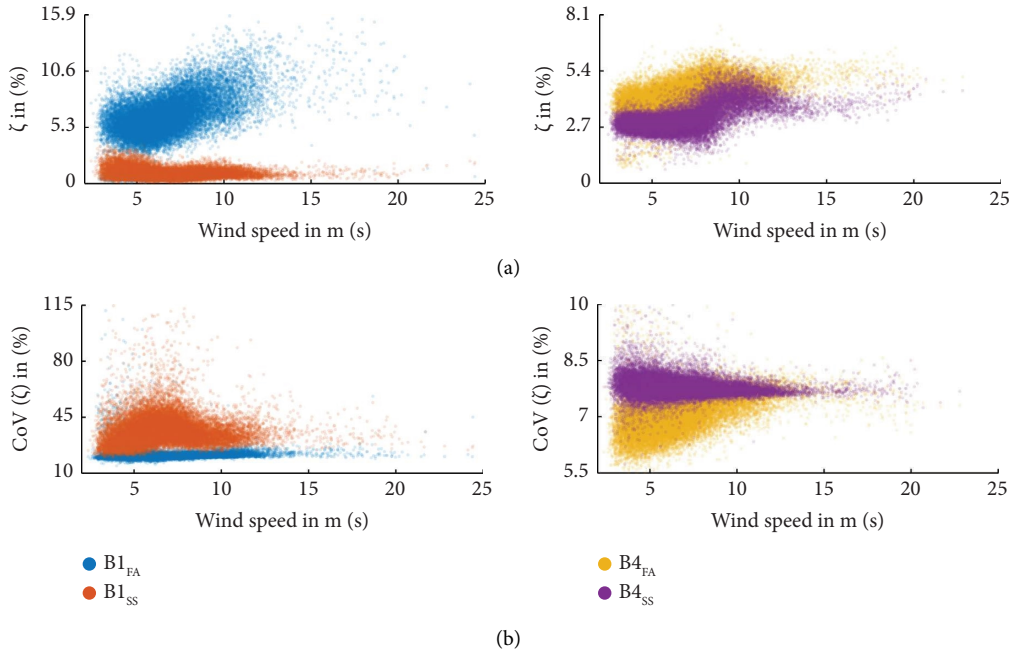

FIGURE 14: (a) Damping ratio of the first and fourth bending mode pairs as a function of wind speed. (b) Coefficient of variation (CoV) of the damping ratio as a function of wind speed.

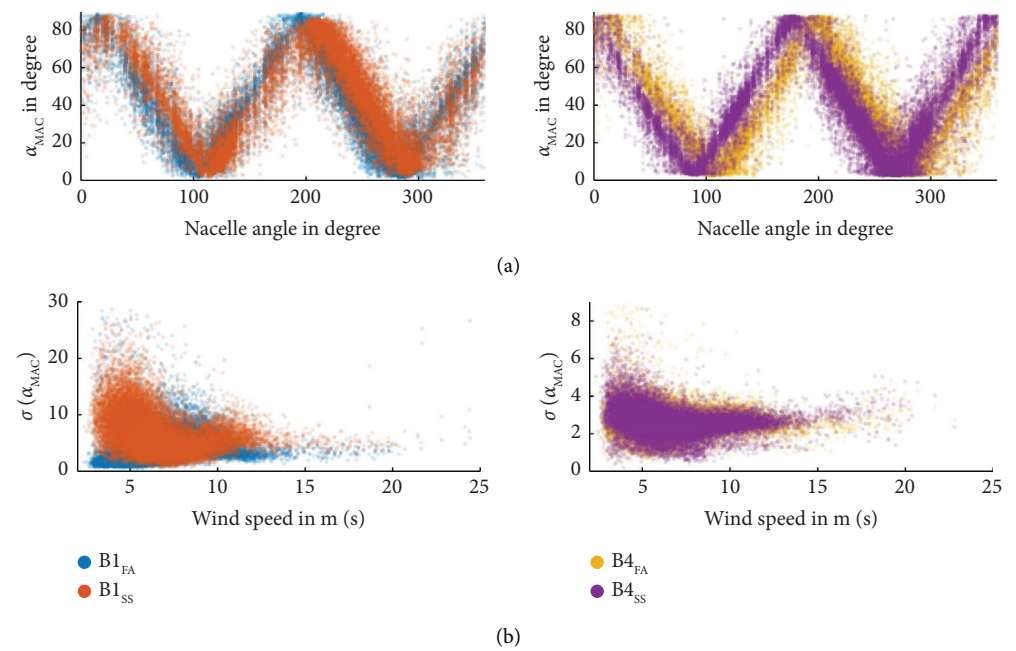

FIGURE 15: (a) α_{MAC} of the first and fourth bending mode pairs as a function of the nacelle angle. (b) Standard deviation of α_{MAC} for the first and fourth bending mode pairs as a function of wind speed.

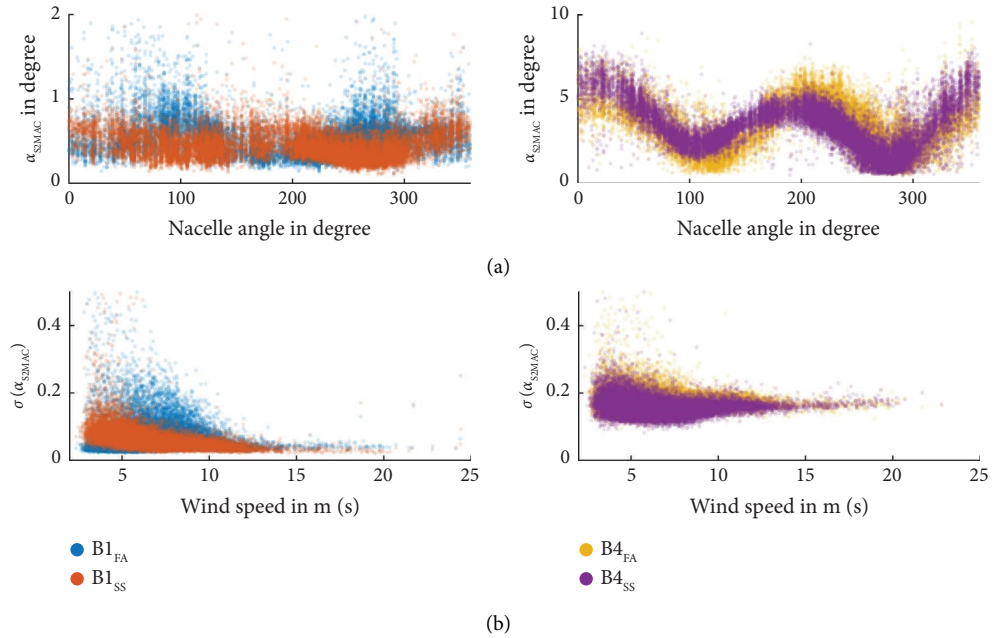

FIGURE 16: (a) α_{S2MAC} of the first and fourth bending mode pairs as a function of the nacelle angle. (b) Standard deviation of α_{S2MAC} for the first and fourth bending mode pairs as a function of wind speed.

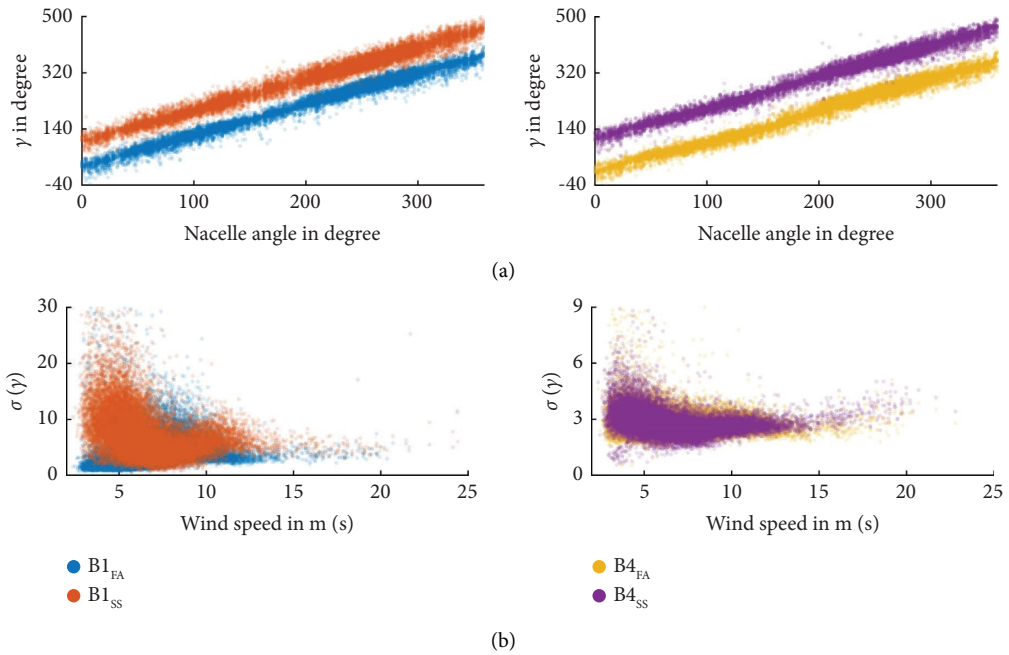

FIGURE 17: (a) Directional angle γ of the first and fourth bending mode pairs as a function of the nacelle angle. (b) Standard deviation of the directional angle γ as a function of wind speed.

6. Summary and Outlook

In this study, the identification uncertainty of modal parameters, especially mode shapes, of a tower of a wind turbine in operation is investigated using BAYOMA. The identification and the corresponding uncertainties provided plausible results despite the presence of harmonic excitation from the rotor. The analysis of identification uncertainties demonstrates that more strongly damped natural frequencies are much more uncertain to identify. Consequently, the less damped natural frequencies in the SS direction can be more reliably identified than the ones in the FA direction. As typical for structures exhibiting closely spaced modes, the mode shapes can only be identified with high uncertainty because the alignment of the mode in the MSS is very uncertain. Therefore, α_{MAC} and the mode alignment angle are not suitable as reliable monitoring parameters. This statement does not apply to α_{S2MAC}, which proved to be a reliable monitoring parameter, as already shown in previous studies for tower structures [21, 25].

Several future research approaches result from this study. For the investigated wind turbine tower, harmonic excitation did not have a significant impact, so identifying the modal parameters with BAYOMA worked well. For a more general statement, it is thus necessary to investigate how harmonic excitation can affect the modal identification of wind turbine support structures constructed exclusively from steel, both onshore and offshore. In addition, a comparison of BAYOMA with the SSI-COV and its uncertainties should be made. In this context, it is crucial to investigate the splitting of the mean phase of the mode shape by spatial direction in the complex plane in the case of closely spaced modes to obtain an interpretation of this behaviour.

The examination of the modal parameters clearly showed that they vary due to EOCs, so the next step is to normalise the data for a reliable SHM scheme. The uncertainties of the modal parameters indicate heteroscedasticity concerning the EOC, i.e., a variability in dependence of the EOCs. Therefore, heteroscedastic Gaussian process regression might be a suitable method for data normalisation to map this variability accurately. The identification results of BAYOMA with their uncertainties can be used in future research to calibrate models considering the uncertainties. This model calibration applies, in particular, to parameters that are difficult to collect, such as soil parameters, to enable realistic soil-structure interactions. Combined with a fluid-structure interaction based on the unsteady vortex lattice method, we aim for more realistic load cases of onshore as well as offshore wind turbines that can be calculated using DeSiO with respect to commonly used wind turbine simulation tools.

Data Availability

The data that have been used are subject of nondisclosure agreement and cannot be published.

Disclosure

A preprint of a previous version is published on a preprint server [42].

Conflicts of Interest

The authors declare that they have no conflicts of interest.

Authors' Contributions

CJ was responsible for conceptualisation and methodology. CJ and SM were responsible for formal analysis. CJ and LL were responsible for investigation and visualisation. CJ, SM, and DS were responsible for original draft preparation. TG and RR were responsible for supervision. SM, LL, DS, BH, TG, and RR were responsible for review and editing. RR was responsible for resources and funding acquisition. All authors have approved the final submitted draft.

Acknowledgments

We are grateful to the *Deutsche WindGuard GmbH* as well as the *Bremer Institut für Messtechnik, Automatisierung und Qualitätswissenschaft* (BIMAQ) for their support during the measurement campaign. This work was supported by the German Research Foundation (SFB 1463-434502799) and the Federal Ministry for Economic Affairs and Climate Action of Germany (research projects Deutsche Forschungsplattform für Windenergie, FKZ 0325936E, and PreciWind-Präzises Messsystem zur berührungslosen Erfassung und Analyse des dynamischen Strömungsverhaltens von WEA-Rotorblättern, FKZ 03EE3013B). Open-access funding was enabled and organized by Projekt DEAL.

References

[1] European Commission and Directorate-General for Environment for Environment, *Guidance Document on Wind Energy Developments and EU Nature Legislation*, Publications Office of the European Union, Luxembourg, 2021.

[2] C. R. Farrar and K. Worden, "An introduction to structural health monitoring," *Philosophical Transactions of the Royal Society A: Mathematical, Physical and Engineering Sciences*, vol. 365, no. 1851, pp. 303–315, 2007.

[3] W. Popko, *Impact of Sea Ice Loads on Global Dynamics of Offshore Wind Turbines*, Fraunhofer Verlag Stuttgart, Germany, 2020.

[4] B. Bozyigit, I. Bozyigit, and L. J. Prendergast, "Analytical approach for seismic analysis of onshore wind turbines considering soil-structure interaction," *Structures*, vol. 51, pp. 226–241, 2023.

[5] S. Adhikari and S. Bhattacharya, "Vibrations of wind-turbines considering soil-structure interaction," *Wind and Structures An International Journal*, vol. 14, no. 2, pp. 85–112, 2011.

[6] C. R. Farrar and K. Worden, *Structural Health Monitoring: A Machine Learning Perspective*, John Wiley & Sons, Hoboken, NJ, USA, 2012.

[7] M. W. Häckell and R. Rolfes, "Monitoring a 5MW offshore wind energy converter—condition parameters and triangulation based extraction of modal parameters," *Mechanical Systems and Signal Processing*, vol. 40, no. 1, pp. 322–343, 2013.

[8] C. Devriendt, F. Magalhães, W. Weijtjens, G. de Sitter, Á. Cunha, and P. Guillaume, "Structural health monitoring of offshore wind turbines using automated operational modal

analysis," *Structural Health Monitoring*, vol. 13, no. 6, pp. 644–659, 2014.

[9] G. Oliveira, F. Magalhães, Á. Cunha, and E. Caetano, "Vibration-based damage detection in a wind turbine using 1 year of data," *Structural Control and Health Monitoring*, vol. 25, no. 11, Article ID e2238, 2018.

[10] C.-H. Loh, K. J. Loh, Y.-S. Yang, W.-Y. Hsiung, and Y.-T. Huang, "Vibration-based system identification of wind turbine system," *Structural Control and Health Monitoring*, vol. 24, no. 3, Article ID e1876, 2017.

[11] R. A. McAdam, M. N. Chatzis, M. Kuleli, E. F. Anderson, and B. W. Byrne, "Monopile foundation stiffness estimation of an instrumented offshore wind turbine through model updating," *Structural Control and Health Monitoring*, vol. 2023, Article ID 4474809, 19 pages, 2023.

[12] C. Koukoura, A. Natarajan, and A. Vesth, "Identification of support structure damping of a full scale offshore wind turbine in normal operation," *Renewable Energy*, vol. 81, no. 8, pp. 882–895, 2015.

[13] N. Penner, T. Grießmann, and R. Rolfes, "Monitoring of suction bucket jackets for offshore wind turbines: dynamic load bearing behaviour and modelling," *Marine Structures*, vol. 72, Article ID 102745, 2020.

[14] W. Weijtjens, G. De Sitter, C. Devriendt, and P. Guillaume, "Automated operational modal analysis on an offshore wind turbine: challenges, results and opportunities," in *6th IOMAC: International Operational Modal Analysis Conference Proceedings*, pp. 713–730, Asturias, Spain, June 2015.

[15] G. Oliveira, F. Magalhães, Á. Cunha, and E. Caetano, "Continuous dynamic monitoring of an onshore wind turbine," *Engineering Structures*, vol. 164, pp. 22–39, 2018.

[16] J. M. W. Brownjohn, A. Raby, S.-K. Au et al., "Bayesian operational modal analysis of offshore rock lighthouses: close modes, alignment, symmetry and uncertainty," *Mechanical Systems and Signal Processing*, vol. 133, Article ID 106306, 2019.

[17] C. Jonscher, B. Hofmeister, T. Grießmann, and R. Rolfes, "Very low frequency IEPE accelerometer calibration and application to a wind energy structure," *Wind Energy Science*, vol. 7, no. 3, pp. 1053–1067, 2022.

[18] S.-K. Au, J. M. Brownjohn, B. Li, and A. Raby, "Understanding and managing identification uncertainty of close modes in operational modal analysis," *Mechanical Systems and Signal Processing*, vol. 147, Article ID 107018, 2021.

[19] S.-K. Au, F.-L. Zhang, and Y.-C. Ni, "Bayesian operational modal analysis: theory, computation, practice," *Computers and Structures*, vol. 126, pp. 3–14, 2013.

[20] M. Döhler and L. Mevel, "Efficient multi-order uncertainty computation for stochastic subspace identification," *Mechanical Systems and Signal Processing*, vol. 38, no. 2, pp. 346–366, 2013.

[21] C. Jonscher, L. Liesecke, N. Penner, B. Hofmeister, T. Grießmann, and R. Rolfes, "Influence of system changes on closely spaced modes of a large-scale concrete tower for the application to structural health monitoring," *Journal of Civil Structural Health Monitoring*, vol. 13, no. 4-5, pp. 1043–1060, 2023.

[22] D. Dooms, G. Degrande, G. de Roeck, and E. Reynders, "Finite element modelling of a silo based on experimental modal analysis," *Engineering Structures*, vol. 28, no. 4, pp. 532–542, 2006.

[23] L. Liesecke, C. Jonscher, T. Grießmann, and R. Rolfes, "Investigations of mode shapes of closely spaced modes from a lattice tower identified using stochastic subspace identification," in *International Conference on Experimental Vibration Analysis for Civil Engineering Structures*, pp. 529–538, Springer, Berlin, Germany, August 2023.

[24] W. D'Ambrogio and A. Fregolent, "Higher-order mac for the correlation of close and multiple modes," *Mechanical Systems and Signal Processing*, vol. 17, no. 3, pp. 599–610, 2003.

[25] C. Jonscher, B. Hofmeister, T. Grießmann, and R. Rolfes, "Influence of environmental conditions and damage on closely spaced modes," in *European Workshop on Structural Health Monitoring*, P. Rizzo and A. Milazzo, Eds., vol. 270, pp. 902–911, Springer, Berlin, Germany, 2023.

[26] C.-X. Qu, T.-H. Yi, H.-N. Li, and B. Chen, "Closely spaced modes identification through modified frequency domain decomposition," *Measurement*, vol. 128, pp. 388–392, 2018.

[27] E. Reynders, J. Houbrechts, and G. de Roeck, "Fully automated (operational) modal analysis," *Mechanical Systems and Signal Processing*, vol. 29, no. 5, pp. 228–250, 2012.

[28] P. Van Overschee and B. De Moor, *Subspace Identification for Linear Systems: Theoryâ–Implementationâ–Applications*, Springer Science & Business Media, Berlin, Germany, 2012.

[29] R. Brincker and P. Andersen, "Understanding stochastic subspace identification," in *Conference Proceedings: IMAC-XXIV: A Conference & Exposition on Structural Dynamics*, Society for Experimental Mechanics, St. Louis, MO, USA, February 2006.

[30] S.-K. Au, "Fast bayesian ambient modal identification in the frequency domain, part i: posterior most probable value," *Mechanical Systems and Signal Processing*, vol. 26, pp. 60–75, 2012.

[31] S.-K. Au, "Connecting bayesian and frequentist quantification of parameter uncertainty in system identification," *Mechanical Systems and Signal Processing*, vol. 29, pp. 328–342, 2012.

[32] C. G. Gebhardt, B. Hofmeister, C. Hente, and R. Rolfes, "Nonlinear dynamics of slender structures: a new object-oriented framework," *Computational Mechanics*, vol. 63, no. 2, pp. 219–252, 2019.

[33] C. G. Gebhardt, I. Romero, and R. Rolfes, "A new conservative/dissipative time integration scheme for nonlinear mechanical systems," *Computational Mechanics*, vol. 65, no. 2, pp. 405–427, 2020.

[34] C. Hente, C. G. Gebhardt, D. Pache, and R. Rolfes, "On the modal analysis of nonlinear beam and shell structures with singular mass and stiffness matrices," *Thin-Walled Structures*, vol. 144, Article ID 106310, 2019.

[35] C. Jonscher, P. Helming, D. Märtins et al., "Dynamic displacement measurement of a wind turbine tower using accelerometers: tilt error compensation and validation," *Wind Energy Science Discussions*, vol. 2023, pp. 1–21, 2023.

[36] J. A. Jimenez Capilla, S.-K. Au, J. M. W. Brownjohn, and E. Hudson, "Ambient vibration testing and operational modal analysis of monopole telecoms structures," *Journal of Civil Structural Health Monitoring*, vol. 11, no. 4, pp. 1077–1091, 2021.

[37] C. Koukoura, A. Natarajan, and A. Vesth, "Identification of support structure damping of a full scale offshore wind turbine in normal operation," *Renewable Energy*, vol. 81, pp. 882–895, 2015.

[38] R. Brincker, P. Andersen, and N.-J. Jacobsen, "Automated frequency domain decomposition for operational modal analysis," in *Proceedings of the 25th SEM International Modal Analysis Conference*, Orlando, FL, USA, February 2007.

[39] F. R. Hampel, "The influence curve and its role in robust estimation," *Journal of the American Statistical Association*, vol. 69, no. 346, pp. 383–393, 1974.

[40] S.-K. Au, *Operational Modal Analysis: Modeling, Bayesian Inference, Uncertainty Laws*, Springer Singapore, Singapore, 1st edition, 2017.

[41] W. Weijtjens, T. Verbelen, G. de Sitter, and C. Devriendt, "Foundation structural health monitoring of an offshore wind turbine—a full-scale case study," *Structural Health Monitoring*, vol. 15, no. 4, pp. 389–402, 2016.

[42] C. Jonscher, S. Möller, L. Liesecke, B. Hofmeister, T. Grießmann, and R. Rolfes, *Bayesian Operational Modal Analysis of Closely Spaced Modes for Monitoring Wind Turbines*, Leibniz University Hannover, Hanover, Germany.